



Microscopic description of structural evolution in Pd, Xe, Ba, Nd, Sm, Gd and Dy isotopes

Tabassum Naz^{1,*}, G. H. Bhat^{2,†}, S. Jehangir^{2,†}, Shakeb Ahmad^{3,+}, J. A. Sheikh^{4,++}

¹*Department of Physics, Aligarh Muslim University, Aligarh, UP - 202 002, India*

²*Department of Physics, S P college, Cluster University Srinagar, 190001, India.*

³*Physics Section, Women's College, Aligarh Muslim University, Aligarh- 202002, India.*

⁴*Cluster University Srinagar, Jammu and Kashmir, 190 001, India*

Abstract

Aiming to understand the role of triaxiality and the evolution of the ground state nuclear shapes, we have carried out a microscopic study for a series of chains of Pd, Xe, Ba, Nd, Sm, Gd, and Dy isotopes. This is done within the self-consistent Relativistic-Hartree-Bogoliubov (RHB) formalism, and supported by the Triaxial Projected Shell Model (TPSM) approach. Pairing interaction separable in the momentum space with DD-ME2 force parameter is used to generate the potential energy surfaces (PESs) under the axial and triaxial symmetry. Shape evolution manifest themselves in very clear manner in almost all the isotopic chains. Properties of the global minima have been found to be in good agreement with the available experimental data. Relatively flat PESs, and γ -soft nature, have been suggested ^{108,110}Pd, ^{132,134}Xe and ¹³⁴Ba as good candidates for E(5) symmetry, while ¹⁰²Pd is not found suitable for E(5) symmetry. The PESs with a bump, and rigidity against triaxial variable(γ) suggested ¹⁵⁰Nd, ¹⁵²Sm and ¹⁵⁴Gd to be good candidates while ¹⁵⁰Sm and ¹⁵⁶Dy are poor candidates of X(5) critical-point symmetry. The findings of the present RHB calculations supported by TPSM are qualitatively in good agreement with the experimental and other theoretical calculations.

© 2015 Published by Elsevier Ltd.

Keywords:

PACS: 25.70.-z, 25.70.Gh, 25.70.Jj, 25.70.Mn

1. INTRODUCTION

Atomic nucleus is one of the most remarkable quantum many-body systems depicting a rich variety of shapes (geometric configurations) within an isotopic/isotonic chain. The single-nucleon shell structure can be dramatically altered with the addition or subtraction of a few nucleons. In some cases, it can also lead to shape transitions within the isotopic/isotonic chain. The transition may occur either from spherical to γ -unstable deformed or from spherical to axially deformed. Understanding the shape, and its modifications near the critical point of the shape phase transition

Email addresses: tabassumnaz321@gmail.com (Tabassum Naz^{1,*}), gwhr.bhat@gmail.com (G. H. Bhat^{2,†}), jehangir@nitsri.net (S. Jehangir^{2,†}), physics.sh@gmail.com (Corresponding author) (Shakeb Ahmad^{3,+}), sjaphysics@gmail.com (J. A. Sheikh^{4,++})

is one of the topical issues in nuclear structure studies. The nuclei around the critical point of the phase transition are characterized by a certain dynamical symmetry. To understand the manifestation of nuclear phase transition and its corresponding critical point dynamical symmetry, many theoretical as well as experimental studies have been done [1]–[49]. These studies were aimed to study the structural evolution along with the possible existence of the two well known dynamical symmetries [E(5) and X(5)] at the critical points of shape phase transitions. The E(5) and X(5) symmetries have been introduced in Refs. [1, 2] in the framework of the Bohr Hamiltonian. E(5) does correspond to the second order shape phase transition seen in the Interacting Boson Model (IBM) between the U(5) and O(6) symmetries, and X(5) does correspond to the first order shape phase transition seen in the IBM between the U(5) and SU(3) symmetries, but the terminology has to differ. Schematically, there are two symmetry triangles: one for the Bohr Hamiltonian, on which E(5) and X(5) appear, and one for the IBM, on which the first and second order transitions appear. The analysis of the structural evolution based on the potential energy surface (PES) leads to the prediction of these symmetries. At the critical point of shape phase transition, the PES of the particular nucleus is expected to be flat-bottom. If the PES of a particular nucleus at the critical point of shape transition may be described by an infinite square well in β -variable, independent of the collective γ -variable then, it is supposed to be a possible candidate for E(5). For X(5), it is assumed that the PES with a bump, and rigidity against triaxial variable (γ) may be described by the sum of an infinite square well and harmonic oscillator.

It is expected and observed that the neutron-rich isotopes of the Pd, Xe, Ba, Nd, Sm, Gd and Dy are located within an interesting region of the nuclear chart. Furthermore, many interesting structural variation are expected which are sensitive to the number of nucleons. Studies aiming to the structural evolution of Pd(Z=46), Xe(Z=54) and Ba(Z=56) isotopes have predicted the shape transition from spherical to deformed nuclei. These studies have also predicted the possible candidates for the critical point symmetry [5, 20, 21, 23, 26, 27][29]–[32][35]. The study, done by Casten and Zamfir [5], has shown the shape transition from spherical to deformed system and proposed ^{134}Ba as the candidate to exhibit the E(5) characteristics. Although, till date, the absolute transition probabilities are not available for a full comparison with the calculations. None of the other nuclei have been found to show a better depiction of such symmetry and hence ^{134}Ba is still considered to be the ideal candidate as supported by other studies [20]. Shape transition has also been observed in Pd isotopes, and ^{102}Pd [21, 23], ^{108}Pd [29, 31, 32] are proposed to be possible candidates for E(5) symmetry. On the basis of a systematic analysis done on the energy level data, B(E2) transition rates [23, 26], and measurements of E1 and M1 strengths of $^{124-136}\text{Xe}$ [27], the shape phase transition around $A \approx 130$ has been demonstrated. These studies along with others have suggested $^{128,130,132}\text{Xe}$ [23, 26, 27, 30, 31, 32, 35] as the possible candidates exhibiting E(5) character. It is known that the isotopes of rare-earth region around $N = 90$ show transitional properties. The isotopes of Nd, Sm, Gd, and Dy are observed to lie in an ideal region of the nuclear chart for the study of shape transition from spherical nuclei at the closed neutron shell at $N=82$ to deformed nuclei. Further study has shown that $N=90$ isotones are the best candidates for X(5) critical-point symmetry [23]. First candidates to display X(5) symmetry were ^{150}Nd [38], ^{152}Sm [39, 40]. This was further supported by other studies done for ^{152}Sm [7, 22, 24, 25] and for ^{150}Nd [7, 24, 28]. Other possible candidates for X(5) symmetry, amongst $N=90$ isotones are ^{154}Gd [43, 44] and ^{156}Dy [18, 44]. It is predicted that, the ^{156}Dy has more γ -soft nature than any other X(5) candidate, yet shows many features of a typical X(5) nucleus ([44, 45] and the references therein).

The purpose of this paper is to investigate the occurrence of the nuclear phase transition, and to search the possible nuclei corresponding to the critical point symmetry. It is known that within the mean-field approach the study of nuclear shape evolution with the number of nucleons is usually done through the potential energy surfaces (PESs). In the present calculations, we have tried to search for the examples of nuclei near the critical-point of the nuclear phase transition based on the PESs. This is done within the Relativistic-Hartree-Bogoliubov (RHB) formalism, supported by the Triaxial Projected Shell Model (TPSM) approach. These studies have been carried out for $^{96-114}\text{Pd}$, $^{128-140}\text{Xe}$, $^{126-142}\text{Ba}$, $^{142-156}\text{Nd}$, $^{144-158}\text{Sm}$, $^{146-158}\text{Gd}$, and $^{148-160}\text{Dy}$ isotopes. Within the isotopic chain we search for the shape transition, and around the critical point for the one with relatively flat PES or PES with a bump as one of the candidates for the critical point symmetry. Further, the triaxial calculation is done to investigate the behaviour of the triaxial parameter γ for those isotopes where the existence of any of the above symmetries is expected. In RHB approach, we have used the density-dependent DD-ME2 [50] parameter set. It provides a successful description of ground state properties [51]–[54] over all the nuclear chart. In order to investigate the high-spin behaviour of the nuclei near the critical points, Triaxial projected shell model (TPSM) approach has been employed. This manuscript is organized as follows. In section 2.1 a general overview of the theoretical formalism is presented. The numerical results of the calculations are discussed and compared in section 3. Summary and conclusions are in section 4.

2. Theoretical Approaches

This present work concerns the microscopic description of the axial and triaxial shapes along with the corresponding ground state properties of neutron-rich Pd, Xe, Ba, Nd, Sm, Gd and Dy isotopes. This has been done within the RHB formalism with density-dependent finite range meson-exchange model. Further study, designed to explore the rotational properties of these systems, is obtained by using the TPSM approach.

2.1. The Meson-exchange Model

In the present calculations the density-dependent finite range meson-exchange model (DD-ME) [50][55]–[58] within the Relativistic-Hartree-Bogoliubov (RHB) formalism is used. The DD-ME model has been used earlier very successfully and have provided an excellent predictions of different ground states and excited state properties throughout the entire periodic table of nuclei [50]–[54][59]–[65]. The present investigation uses the very successful, density-dependent meson-exchange DD-ME2 [50] parameter set. The pairing correlation is taken care within a pairing interaction separable in momentum space. For the details of the calculations see Refs. [59]–[61][66]–[71]. The potential energy surface (PES) calculation is done by imposing constraints on both axial and triaxial mass quadrupole moments. It is performed by the method of quadratic constrained [67] by using an unrestricted variation of the function

$$\langle \hat{H} \rangle + \sum_{\mu=0,2} C_{2\mu} (\langle \hat{Q}_{2\mu} \rangle - q_{2\mu})^2 \quad (1)$$

where $\langle \hat{H} \rangle$ is the total energy, $\langle \hat{Q}_{2\mu} \rangle$ denotes the expectation values of mass quadrupole operators,

$$\hat{Q}_{20} = 2z^2 - x^2 - y^2 \quad \text{and} \quad \hat{Q}_{22} = x^2 - y^2 \quad (2)$$

$q_{2\mu}$ is the constrained value of the multipole moment, and $C_{2\mu}$ is the corresponding stiffness constant. Moreover, the quadratic constraint adds an extra force term $\sum_{\mu=0,2} \lambda_{\mu} \hat{Q}_{2\mu}$ to the system, where

$$\lambda_{\mu} = 2C_{2\mu} (\langle \hat{Q}_{2\mu} \rangle - q_{2\mu}) \quad (3)$$

for a self consistent solution. This term is necessary to force the system to a point in deformation space different from a stationary point. The convergence of the numerical calculation is taken care properly in terms of the optimum numbers of oscillator quanta for fermions and bosons.

2.2. Triaxial Projected Shell Model Approach

It has been demonstrated recently that multi-quasiparticle triaxial projected shell model (TPSM) approach provides a coherent description of yrast, γ and multi-quasiparticle band structures in transitional nuclei [72]–[75]. In this approach, three dimensional projection technique is employed to project out the good angular-momentum states from triaxially deformed Nilsson + BCS basis. Shell model Hamiltonian is subsequently diagonalized using these angular-momentum projected basis states [76]–[79]. As in the earlier PSM calculations, we use the pairing plus quadrupole-quadrupole Hamiltonian [80]

$$\hat{H} = \hat{H}_0 - \frac{1}{2}\chi \sum_{\mu} \hat{Q}_{\mu}^{\dagger} \hat{Q}_{\mu} - G_M \hat{P}^{\dagger} \hat{P} - G_Q \sum_{\mu} \hat{P}_{\mu}^{\dagger} \hat{P}_{\mu}, \quad (4)$$

Where χ is the interaction strength of the QQ-force. The monopole pairing strength G_M is of the standard form

$$G_M = \frac{G_1 - G_2 \frac{N-Z}{A}}{A} \text{ for neutrons, } G_M = \frac{G_1}{A} \text{ for protons.} \quad (5)$$

In the present work, we consider $G_1 = 20.12$ and $G_2 = 13.13$, which approximately reproduce the observed odd-even mass difference. and this choice of G_M is appropriate for the single-particle space employed in the model, where three major shells are used for each type of nucleons ($N = 4, 5, 6$ ($N = 3, 4, 5$) and $3, 4, 5$ ($2, 3, 4$) for neutrons (protons) for $A \sim 160$ and $A \sim 130$ regions respectively). The quadrupole pairing strength G_Q is assumed to be proportional to G_M , and the proportionality constant being set equal to 0.16 [72]–[75].

3. Results and Discussion

3.1. Relativistic-Hartree-Bogoliubov(RHB) with density-dependent finite range meson-exchange model

In this section, we present the microscopic description of Pd(Z=46), Xe(Z=54), Ba(Z=56), Nd(Z=60), Sm(Z=62), Gd(Z=64), and Dy(Z=66) isotopic chains. We have performed the constrained calculations to obtain the axial as well as the triaxial potential energy surfaces(PESs). The effective interaction used is density-dependent DD-ME2.

3.1.1. Axial Symmetry

In Fig. 1, we display the PESs of $^{96-114}\text{Pd}$, $^{128-140}\text{Xe}$, and $^{126-142}\text{Ba}$ as a function of the quadrupole deformation β_2 . From these figures, one can observe the shape transition from the spherical ^{96}Pd (N=50) to the γ -unstable(prolate) ^{108}Pd (N=62), then to the γ -unstable(oblate) $^{110-114}\text{Pd}$ (N=62-68) isotopes. Similar shape phase transition can be seen from Xe isotopes. But, in this case the shape transition can be seen for either side of the spherical ^{136}Xe (N=82) to the γ -unstable(prolate) ^{128}Xe (N=62) and towards neutron increasing ^{140}Xe (N=86). The same behaviour is there in case of Ba isotopes, from spherical ^{138}Ba (N=82) to the γ -unstable(prolate) ^{126}Ba (N=70). In Fig. 1(a), we can see the shape coexistence in almost all the isotopes of Pd(Z=46) with an energy difference between prolate and oblate around 0.5MeV(minimum) for ^{108}Pd , and about 3MeV(maximum) for ^{102}Pd . Just at the critical point of shape transition from prolate (^{108}Pd) to oblate (^{110}Pd), the PESs of ^{108}Pd and $^{110-114}\text{Pd}$ are quite flat among all the Pd isotopes. In Fig. 1(b), at $^{132,134}\text{Xe}$ and ^{138}Xe , the PESs has a flat bottom ($\leq 0.75\text{MeV}$ energy difference), and transition occurs from deformed to spherical and from spherical to deformed respectively. The PES of $^{134,138}\text{Xe}$ is more flat than ^{132}Xe . In case of Ba isotopes, shown in Fig. 1(c), the shape coexistence is found in all isotopes except in ^{138}Ba . A relative flat PES is found in ^{134}Ba , covering $0.1 \leq |\beta_2| \leq 0.15$.

Now, we present our results for the isotopic chains of some rare-earth nuclei, Nd(Z=60), Sm(Z=62), Gd(Z=64), and Dy(Z=66). The PESs for $^{142-156}\text{Nd}$, $^{144-158}\text{Sm}$, $^{146-158}\text{Gd}$, and $^{148-160}\text{Dy}$ isotopes are shown in Fig. 2. In Fig. 2(a), the ^{142}Nd is spherical and as the neutron number increases, shape transition towards a well deformed prolate minimum can be seen. The isotopes $^{152-156}\text{Nd}$ show a well-deformed prolate minimum. The nucleus ^{144}Nd is having a flat minimum within $-0.1 \leq |\beta_2| \leq 0.1$. Shape coexistence with a small potential barrier of $\sim 1.5\text{MeV}$ and excitation energy of $\sim 0.70\text{MeV}$ can be seen in ^{146}Nd nucleus. The isotopes ^{148}Nd (N=88) and ^{150}Nd (N=90) both lie in the transition region from spherical shape to a well-deformed shape. But, ^{150}Nd is exhibiting a rather flat minimum than ^{148}Nd in the prolate regime, and shallower minimum in the oblate regime. ^{148}Nd has a deep prolate minimum and a shallow oblate minimum with 2.3MeV excitation energy, and, the energy barrier of 4MeV. However, ^{150}Nd has a rather flat potential energy surface on the prolate side $0.2 \leq \beta_2 \leq 0.4$, and shallow oblate minimum at the excitation energies 2.6MeV with 6MeV of the energy barrier. Similar transitional behavior can be seen in PESs for $^{144-158}\text{Sm}$ isotopes (Z=62) shown in Fig. 2(b). We have transition from spherical ^{144}Sm to clear prolate shape $^{154-158}\text{Sm}$ isotopes. The isotopes $^{146,148}\text{Sm}$ is showing the shape coexistence, and the transitional behavior appears for ^{150}Sm (N=88) and ^{152}Sm (N=90). For Gd(Z=64) and Dy(Z=66) isotopes, PESs are shown in Figs. 2(c) and (d), respectively, the same is true. The isotopes ^{154}Gd (N=90) and ^{156}Dy (N=90) show a flat minimum in $\beta_2 > 0$ regime and shallower minimum in $\beta_2 < 0$ regime being in between the transition from spherical to well-deformed prolate shape. The observation of flat potential energy surfaces within these isotopic chains, motivated us to explore their triaxial character.

3.1.2. Triaxial Symmetry

The role of triaxiality becomes important due to the flatness in PESs leading to locate the exact global minimum for such cases. To study the dependency on γ , a systematic constrained triaxial calculation have been done for mapping the quadrupole deformation space defined by β_2 and γ using DD-ME2 effective interaction. Energies are normalized with respect to the binding energy of the global minimum. In Fig.3, Fig.4 and Fig.5 we have displayed the contour plots for $^{96-114}\text{Pd}$, $^{128-140}\text{Xe}$, and $^{126-142}\text{Ba}$, respectively. The ground state quadrupole deformations in the β_2 - γ plane corresponding to the global minima of the triaxial PES are tabulated in Table 1. Table 1, also display the difference in the ground state energies (ΔE_{tr}) as the triaxial deformation energy, with respect to the ground state energies (E_{ax}) corresponding to the axial symmetry. We can see the shape transition is very evident, starting from the spherical(^{96}Pd) to prolate($^{98-104}\text{Pd}$) deformation, and to triaxial($^{106-112}\text{Pd}$) deformation then, shifted to oblate(^{114}Pd) deformation. The PESs appears to be quite γ -soft extended from prolate to oblate, and then starts to become slightly rigid in γ direction towards oblate side. Further, the softness in γ direction is shifting to prolate side. The nucleus ^{106}Pd has two minima at $(0.2, 15^\circ)$ and at $(0.4, 5^\circ)$ with energy difference of 1.21MeV, and the deepest one is $(0.2, 15^\circ)$.

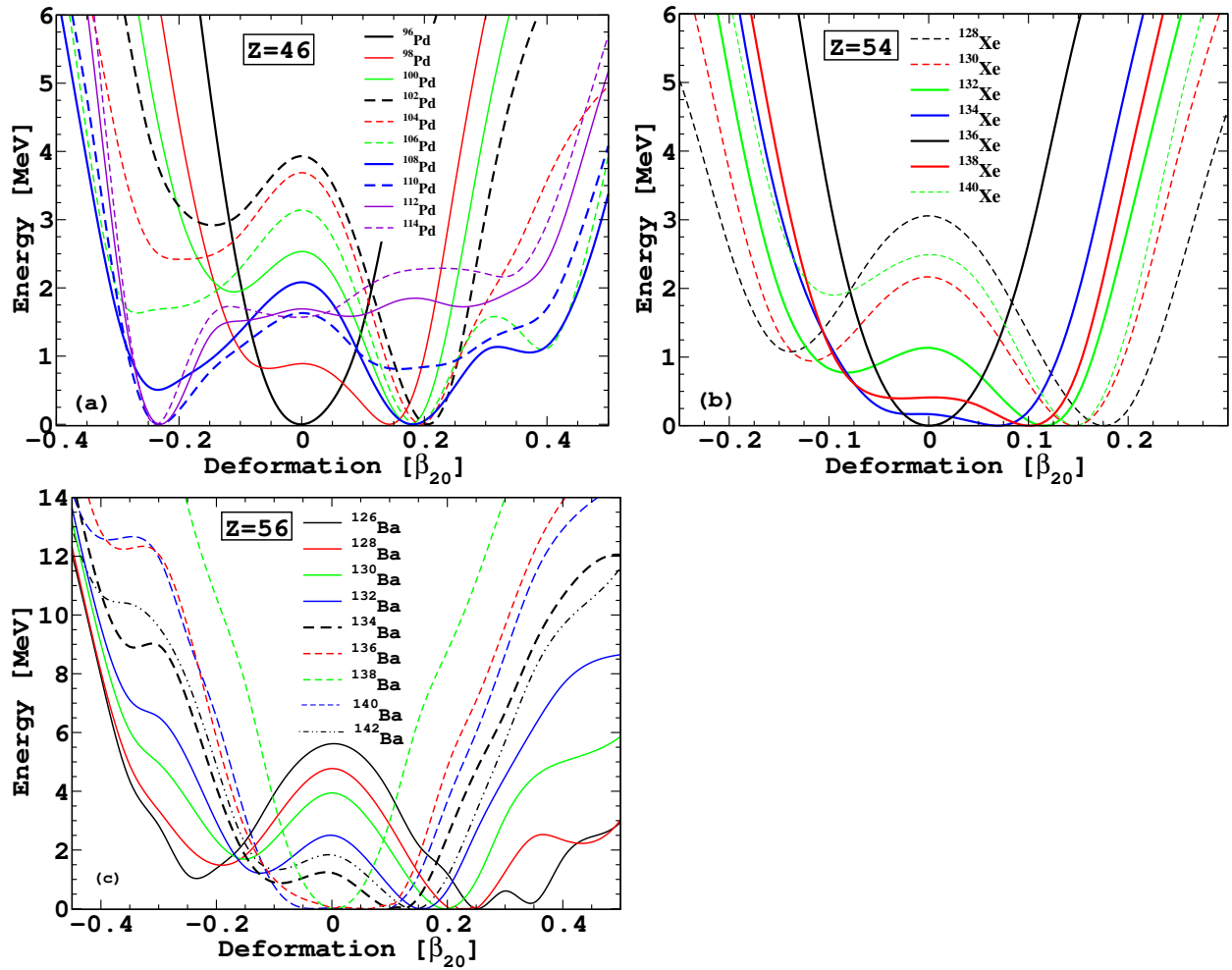


Figure 1. (Color online) Potential energy surfaces(PESs) for (a) $^{96-114}\text{Pd}$, (b) $^{128-140}\text{Xe}$, (c) and $^{126-142}\text{Ba}$, calculated using the RHB theory with the DD-ME2 force. Thick lines corresponds to the possible isotopes that have been suggested to show E(5) critical-point symmetry.

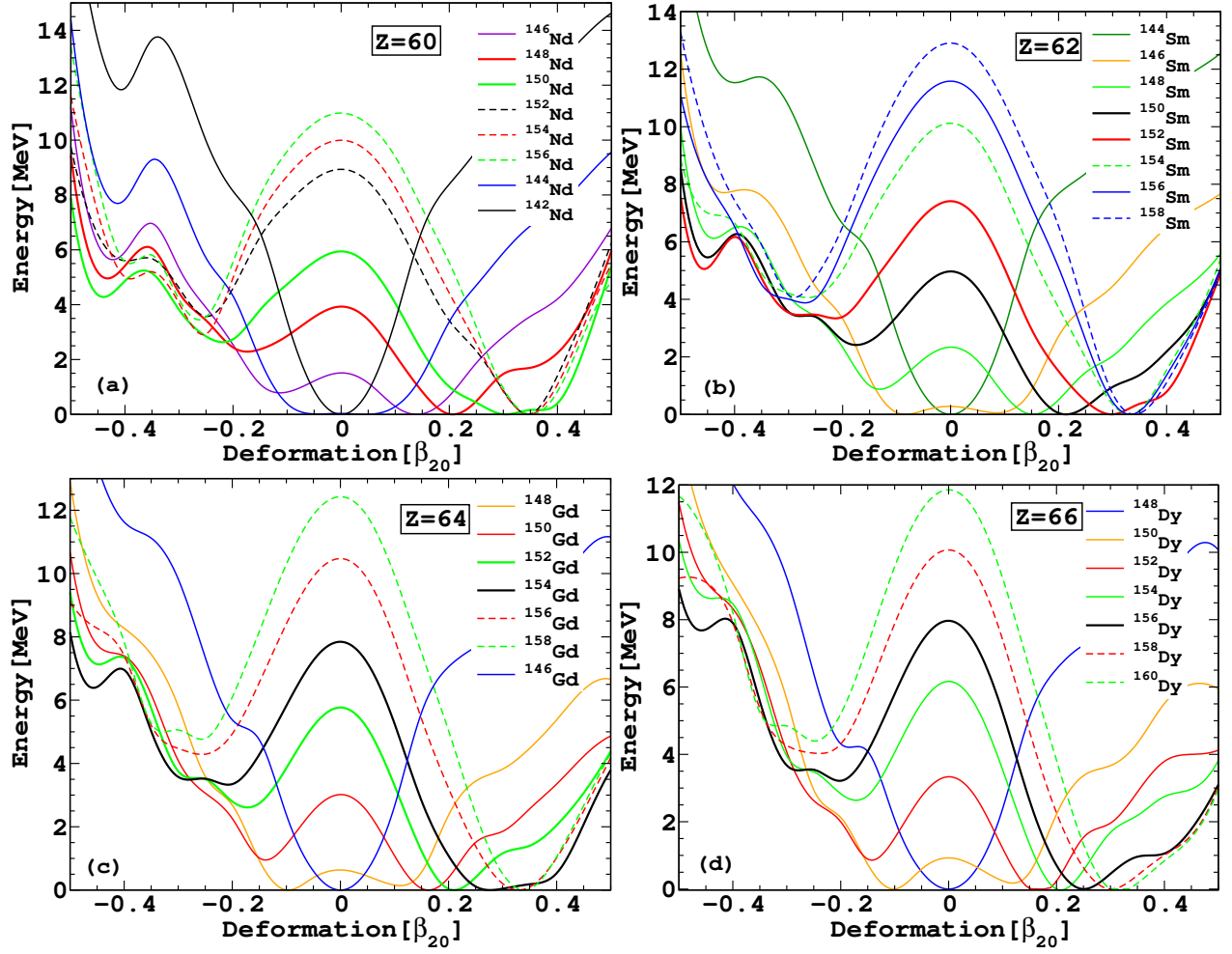


Figure 2. (Color online) Potential energy surfaces(PESs) for (a) $^{142-156}\text{Nd}$, (b) $^{144-158}\text{Sm}$, (c) $^{146-158}\text{Gd}$, and (d) $^{148-160}\text{Dy}$, calculated using the RHB theory with the DD-ME2 force. Thick lines corresponds to the possible isotopes that have been suggested to show X(5) critical-point symmetry.

Similarly, ^{108}Pd has two minima at $(0.25, 25^\circ)$ and at $(0.35, 15^\circ)$ with energy difference of 1.10 MeV, and $(0.25, 25^\circ)$ as the global minimum. Finally, it becomes flat along γ direction towards prolate side at ^{106}Pd . The nucleus $^{108,110}\text{Pd}$ besides triaxiality are showing the γ -soft nature too, favoring larger deformations β on the prolate side ($\gamma = 0^\circ$) and smaller on the oblate side ($\gamma = 60^\circ$). In case of Xe($Z=54$) isotopes, the deformation shifts from prolate to spherical at ^{136}Xe , and then shifts to prolate deformation. Here also the PESs appears to be soft in the γ -direction. The continuous γ -soft behaviour extended from prolate to oblate. These nuclei except ^{136}Xe are not spherical but, rather, characterized by some degree of triaxiality. For Ba($Z=56$) isotopes, the nuclei ^{136}Ba and ^{138}Ba both are of spherical shape. But ^{138}Ba show more spherical character because here the γ -softness is concentrated within smaller β -values. Either side of ^{138}Ba , the deformation is prolate, except at ^{132}Ba , where, triaxiality appears at $(0.15, 15^\circ)$. The nucleus ^{126}Ba being prolate at global minimum, also showing triaxial character at $(0.25, 35^\circ)$ with energy difference of 0.287 MeV. ^{128}Ba nucleus is also showing two coexisting prolate minimum at $(0.2, 0^\circ)$ and $(0.45, 0^\circ)$ with energy difference of 1.89 MeV.

Table 1. The quadrupole deformation (β_2, γ) of the global minima in Pd, Xe and Ba isotopes, calculated within the RHB formalism with DD-ME2. E_{ax} and E_{tr} are the total energies for the global minima under axial and triaxial symmetry, respectively.

Nuclei	β_2	γ	E_{tr}	E_{ax}	ΔE_{tr}	Nuclei	β_2	γ	E_{tr}	E_{ax}	ΔE_{tr}
^{96}Pd	0	0°	815.274	814.972	0.302	^{134}Xe	0.05	0°	1127.397	1127.242	0.155
^{98}Pd	0.15	0°	834.281	834.093	0.187	^{136}Xe	0.0	0°	1143.737	1143.495	0.242
^{100}Pd	0.15	0°	853.584	853.418	0.165	^{138}Xe	0.1	0°	1150.590	1150.329	0.261
^{102}Pd	0.2	0°	872.483	872.518	-0.035	^{140}Xe	0.15	0°	1158.992	1158.743	0.249
^{104}Pd	0.2	0°	889.450	889.400	0.050	^{126}Ba	0.25	0°	1052.447	1052.811	-0.364
^{106}Pd	0.2	15°	905.683	905.520	0.163	^{128}Ba	0.2	0°	1071.578	1071.920	-0.342
^{108}Pd	0.25	25°	921.398	920.673	0.725	^{130}Ba	0.2	0°	1090.329	1090.503	-0.174
^{110}Pd	0.25	35°	936.362	935.772	0.589	^{132}Ba	0.15	15°	1110.230	1108.204	2.026
^{112}Pd	0.25	40°	950.708	950.433	0.274	^{134}Ba	0.16	0°	1127.783	1125.765	2.018
^{114}Pd	0.25	60°	963.820	964.191	-0.370	^{136}Ba	0.0	0°	1143.900	1142.992	0.908
^{128}Xe	0.2	15°	1078.713	1078.666	0.047	^{138}Ba	0.0	0°	1161.120	1161.884	-0.764
^{130}Xe	0.15	10°	1095.489	1095.467	0.022	^{140}Ba	0.1	0°	1170.622	1168.762	1.860
^{132}Xe	0.1	0°	1111.620	1111.449	0.170	^{142}Ba	0.15	0°	1181.460	1178.140	3.320

In Fig.6, Fig.7, Fig.8, and Fig.9 we display the calculated PESs under triaxial symmetry for Nd($Z=60$), Sm($Z=62$), Gd($Z=64$), and Dy($Z=66$) isotopes, respectively. We discuss the shape transition and the properties corresponding to the global minima for $^{142-156}\text{Nd}$, $^{144-158}\text{Sm}$, $^{146-158}\text{Gd}$, and $^{148-160}\text{Dy}$ isotopes. The ground state quadrupole deformations in the β_2 - γ plane corresponding to the global minima of the triaxial PESs are tabulated in Table 2. The nucleus ^{142}Nd is spherical, but ^{144}Nd is slightly triaxial with its global minimum at $(0.05, 5^\circ)$. Further, it is shifting towards higher and higher prolate deformation. For ^{144}Nd and ^{146}Nd , the γ -softness is there covering prolate to oblate region. But as we move further the γ -softness shifted towards the prolate region and becomes rigid towards the oblate region. There is a flat character in γ -softness towards prolate region in ^{150}Nd , after then it concentrates. The ground state of ^{150}Nd nucleus is axially prolate($0.3, 0^\circ$). The convergence of circles around the ground state covers β_2 from 0.15 to 0.45, and the softness in γ is just 10° up to 1.2 MeV of energy. Similar behaviour can be seen in case Sm($Z=62$) isotopes. ^{144}Sm is spherical in shape, and as we move further the shape is shifting towards larger prolate deformation. γ -softness is there in ^{146}Sm and ^{148}Sm , but it shifted towards more prolate region and becomes rigid towards the oblate region. The nuclei, $^{150}\text{Sm}(0.2, 0^\circ)$, $^{152}\text{Sm}(0.3, 0^\circ)$, have their ground state as axially prolate. The convergence of the circles around their global minimum in general, covers the β_2 space from 0.15 to 0.45. But, the γ -softness is different for them. It is 35° up to 1.86 MeV of energy for ^{150}Sm , 15° up to 1.9 MeV for ^{152}Sm . In case of Gd($Z=64$) and Dy($Z=66$) isotopes, we can see exactly the same behaviour in the shape transition as in case of Nd($Z=60$) and Sm($Z=62$). The only difference is that after the spherical global minima in case of ^{146}Gd and ^{148}Dy , the nuclei ^{148}Gd and ^{150}Dy is having the oblate global minimum. The nuclei $^{154}\text{Gd}(0.3, 0^\circ)$, and $^{156}\text{Dy}(0.25, 0^\circ)$ have their ground state as axially prolate, and circles around their global minimum covers the β_2 space from 0.15 to 0.45. The γ -softness is 15° up to 1.55 MeV for ^{154}Gd , and 30° up to 1.9 MeV for ^{156}Dy . Here, the nuclei ^{150}Sm and ^{156}Dy show more γ -soft nature than others. It is in agreement with the experiment reporting more γ -soft behaviour of ^{156}Dy amongst the

N=90 isotones [45]. In general all these nuclei show flatness around their global minimum within the energy range 0 - 2.5MeV approximately in the axially prolate ($0.15 \leq \beta_2 \leq 0.45$) regime effectively, thus reflecting the axial PES behaviour.

Table 2. The quadrupole deformation (β_2 , γ) of the global minima in Nd, Sm, Gd and Dy isotopes, calculated within the RHB formalism with DD-ME2. E_{ax} and E_{tr} are the total energies for the global minima under axial and triaxial symmetry, respectively.

Nuclei	β_2	γ	E_{tr}	E_{ax}	ΔE_{tr}	Nuclei	β_2	γ	E_{tr}	E_{ax}	ΔE_{tr}
¹⁴² Nd	0	0°	1187.941	1187.647	0.294	¹⁴⁴ Sm	0	0°	1197.203	1197.306	-0.103
¹⁴⁴ Nd	0.05	5°	1198.508	1198.220	0.288	¹⁴⁶ Sm	0.1	0°	1209.314	1209.354	-0.039
¹⁴⁶ Nd	0.15	0°	1210.364	1210.119	0.245	¹⁴⁸ Sm	0.15	0°	1223.253	1223.204	0.049
¹⁴⁸ Nd	0.20	0°	1223.080	1222.847	0.232	¹⁵⁰ Sm	0.2	0°	1237.640	1237.350	0.290
¹⁵⁰ Nd	0.3	0°	1235.211	1235.002	0.200	¹⁵² Sm	0.3	0°	1251.460	1251.207	0.253
¹⁵² Nd	0.35	0°	1248.070	1247.891	0.178	¹⁵⁴ Sm	0.35	0°	1265.250	1264.900	0.350
¹⁵⁴ Nd	0.35	0°	1258.760	1258.550	0.210	¹⁵⁶ Sm	0.35	0°	1277.534	1277.171	0.363
¹⁵⁶ Nd	0.35	0°	1269.134	1268.802	0.332	¹⁵⁸ Sm	0.35	0°	1289.398	1289.000	0.397
¹⁴⁶ Gd	0	0°	1204.987	1205.163	-0.175	¹⁴⁸ Dy	0	0°	1211.099	1211.300	-0.200
¹⁴⁸ Gd	0.1	60°	1218.817	1218.812	0.005	¹⁵⁰ Dy	0.1	60°	1226.543	1266.496	0.046
¹⁵⁰ Gd	0.15	0°	1234.344	1234.311	0.033	¹⁵² Dy	0.15	0°	1243.477	1243.483	-0.006
¹⁵² Gd	0.2	0°	1250.100	1249.914	0.185	¹⁵⁴ Dy	0.2	0°	1260.620	1260.453	0.167
¹⁵⁴ Gd	0.3	0°	1264.934	1264.611	0.322	¹⁵⁶ Dy	0.25	0°	1276.499	1276.164	0.335
¹⁵⁶ Gd	0.35	0°	1279.948	1279.533	0.415	¹⁵⁸ Dy	0.3	0°	1292.187	1291.851	0.336
¹⁵⁸ Gd	0.35	0°	1293.963	1293.516	0.446	¹⁶⁰ Dy	0.3	0°	1307.106	1306.771	0.335

3.1.3. Physical properties of global minima

In Figures 10, 11, 12, and 13, we present the physical properties such as binding energies, two neutron separation energies, charge radii and isotopic shifts of the ground state charge radii. These observables can be measured experimentally, and we have compared these observables with experimental values. The binding energies have been presented in Table:1 and Table:2 calculated using axial and triaxial symmetry. In these figures, physical properties presented are by the triaxial calculations. From these figures, we can see the deviation of the calculated triaxial binding energies with respect to the experimental values are around 0.5MeV for most of the cases to a maximum of around 3.5MeV. In case of Xe, ba, Nd, Sm, Gd and Dy isotopes, the sharp kink at N=82 can be seen in two neutron separation energy, as N=82 being neutron closed shell number. It is also observed in charge radii as well as in the isotopic shifts of the ground state charge radii. In general, we can say that the calculated numerical values as well their behaviour is overall in good agreement with available experimental data.

3.1.4. E(5) and X(5) Critical Point Symmetry

The possible candidates of the E(5) critical-point symmetry based on the calculations assuming axial symmetry can be explored by analyzing the flat regions in the axial PESs. In our axial calculations, the relatively flat axial PESs exhibited by ^{108,110}Pd, ^{132,134,138}Xe, and ¹³⁴Ba as shown in Fig. 1, it is evident that, these are transitional nuclei, and can be described assuming infinite square well potential in β -variable. These can be the possible candidates for the E(5) critical-point symmetry. Our findings of ^{108,110}Pd, ^{132,134,138}Xe, and ¹³⁴Ba nuclei to be possible E(5) candidates are in agreement with many theoretical and experimental studies [5, 29, 31, 32, 35]. However, in the present calculation, ¹⁰²Pd is not showing a flat PES. So, it cannot be considered as a possible candidate for E(5). This is not in agreement with the earlier predictions [21, 23, 31]. But, our result is in agreement with the very recent experiment based on lifetime measurements of yrast and non-yrast states of ¹⁰²Pd through a Recoil Distance Doppler Shift(RDDS) [36]. We also know that, from N=90 nuclei, ¹⁵⁰Nd, ¹⁵²Sm, ¹⁵⁴Gd and ¹⁵⁶Dy have been predicted and identified to exhibit the best possible candidates for X(5) critical-point symmetry [6, 18, 22, 24, 25, 28, 38, 40, 43, 44, 45]. The X(5) symmetry corresponds to first order phase transition from a spherical shape to a well-deformed prolate (γ -unstable) shape. The present observations from the axial PESs for ^{142–156}Nd, ^{144–158}Sm, ^{146–158}Gd, and ^{148–160}Dy isotopes shown in Fig. 2, we can notice the possible candidates for X(5) critical-point symmetry. These are ¹⁵⁰Nd, ^{150,152}Sm,

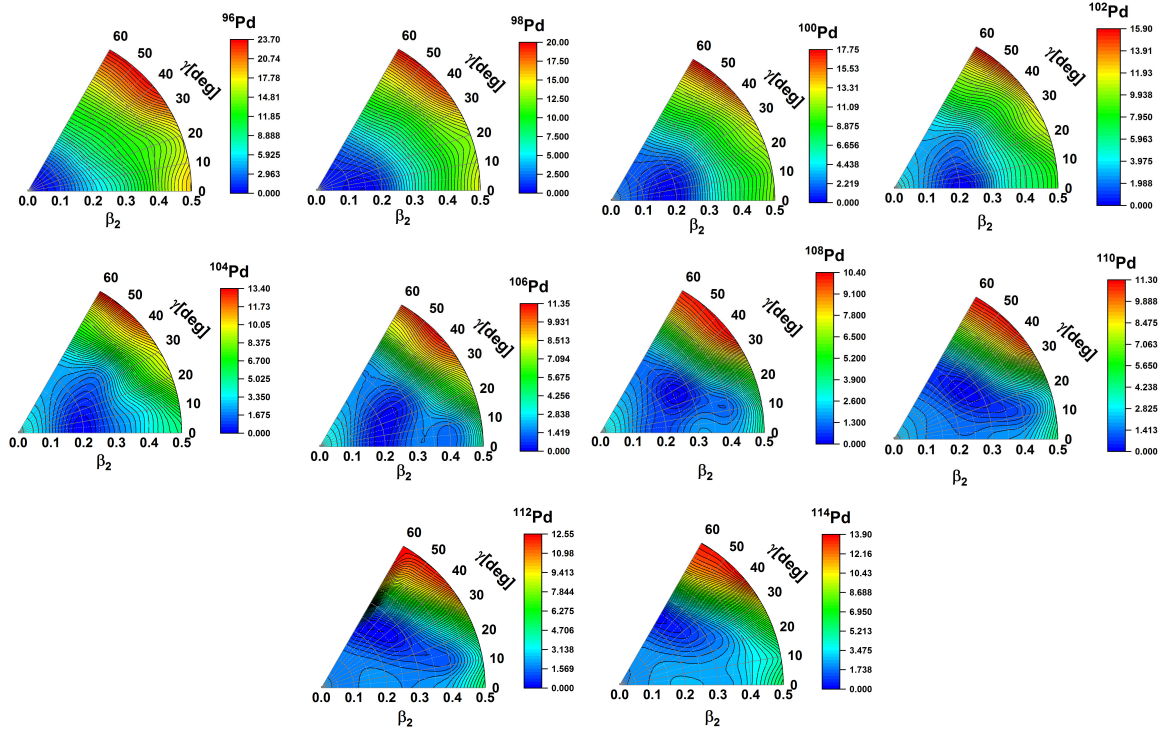


Figure 3. (Color online) Mean field potential energy surfaces for the nuclei $^{96-114}\text{Pd}$ in the (β, γ) plane, obtained from a triaxial RHB calculations with the DD-ME2 parameter set. The color scale shown at the right has the unit of MeV, and scaled such that the ground state has a zero MeV energy.

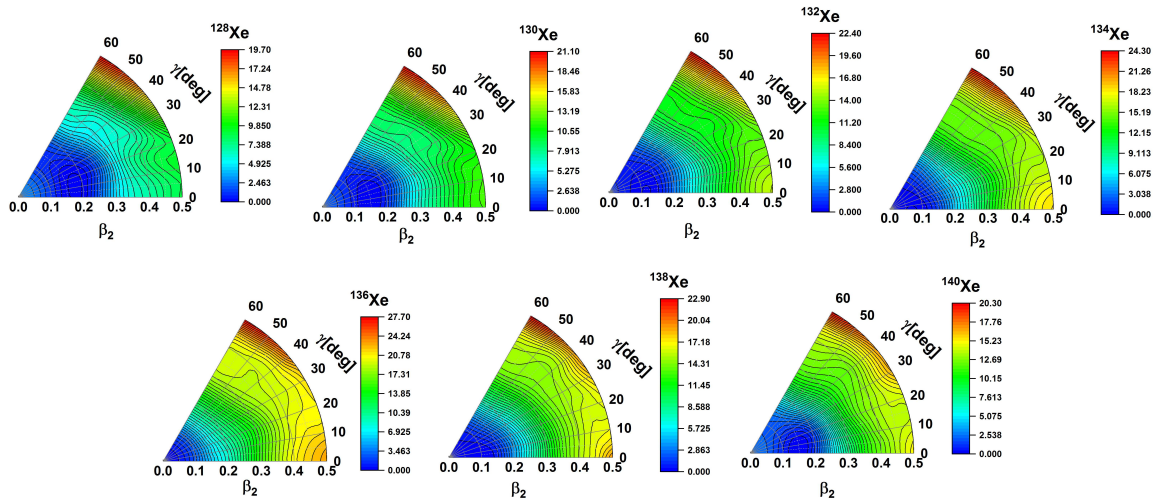


Figure 4. (Color online) Same as Fig.3 for the nuclei $^{128-140}\text{Xe}$.

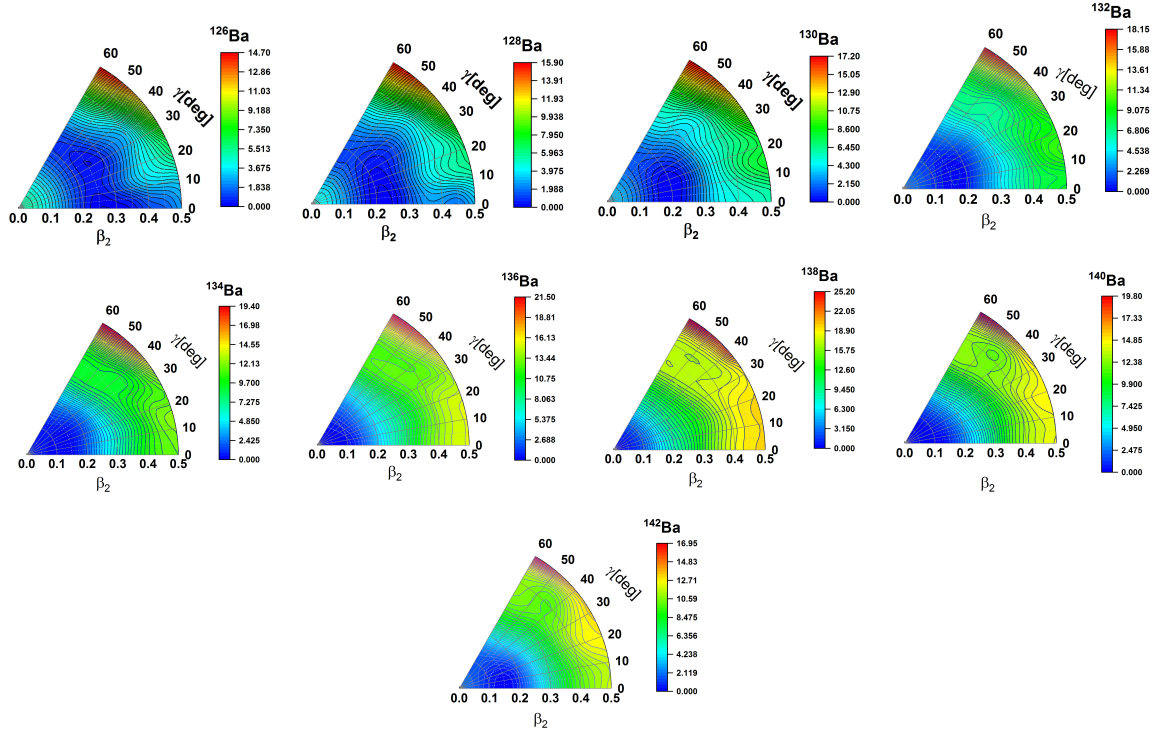


Figure 5. (Color online) Same as Fig.3 for the nuclei $^{126-142}\text{Ba}$.

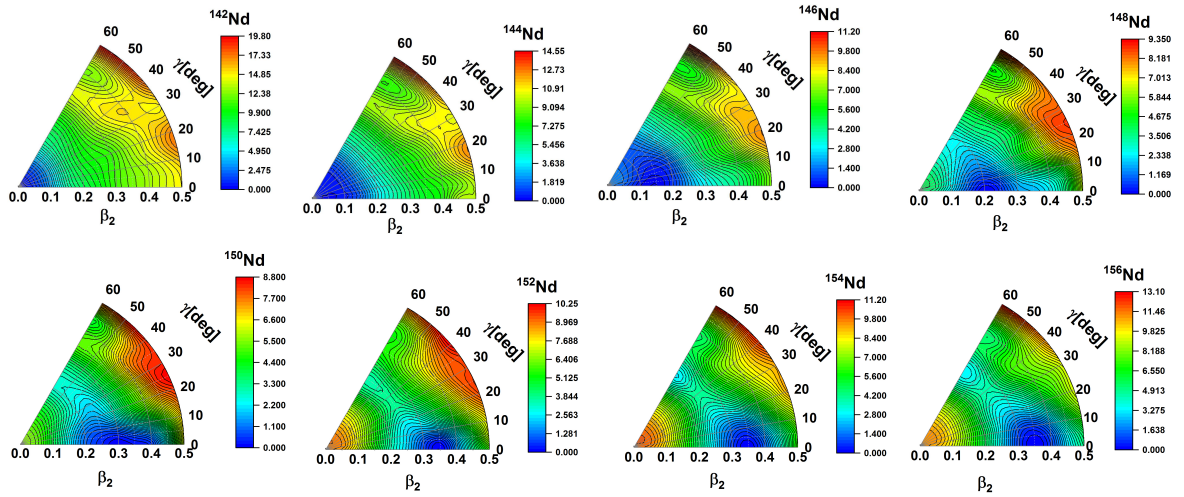


Figure 6. (Color online) Same as Fig.3 for the nuclei $^{142-156}\text{Nd}$.

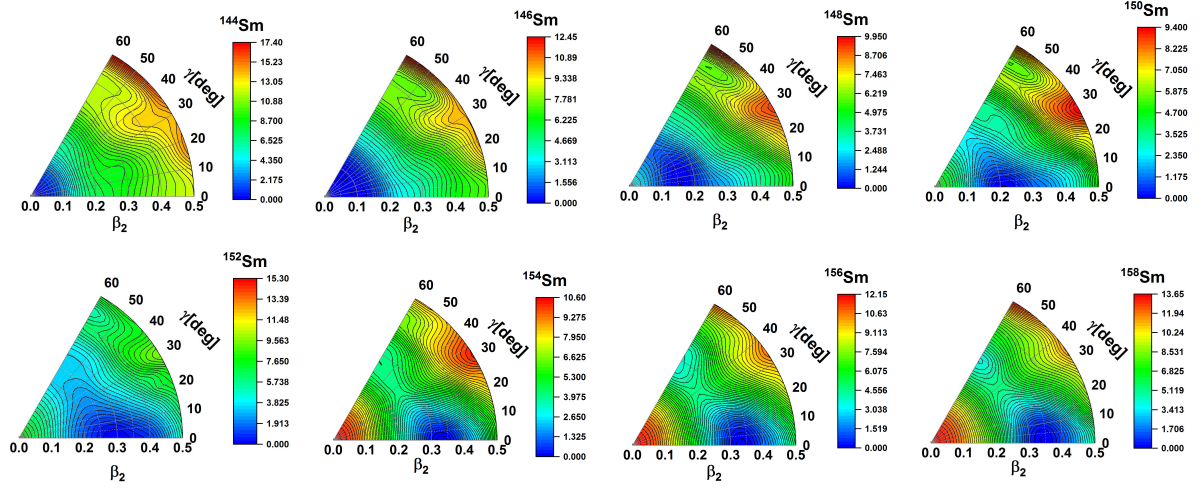


Figure 7. (Color online) Same as Fig.3 for the nuclei $^{144-158}\text{Sm}$.

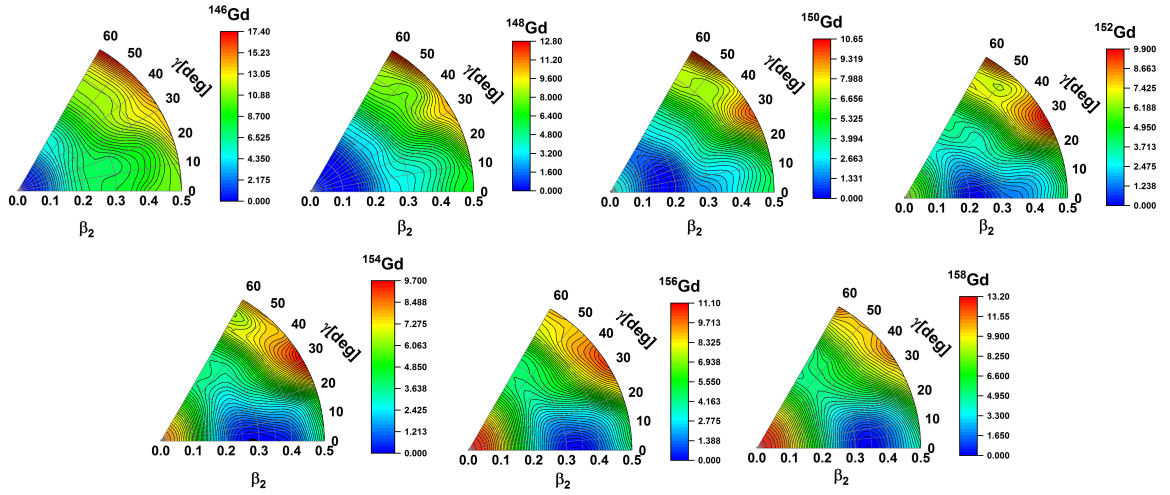
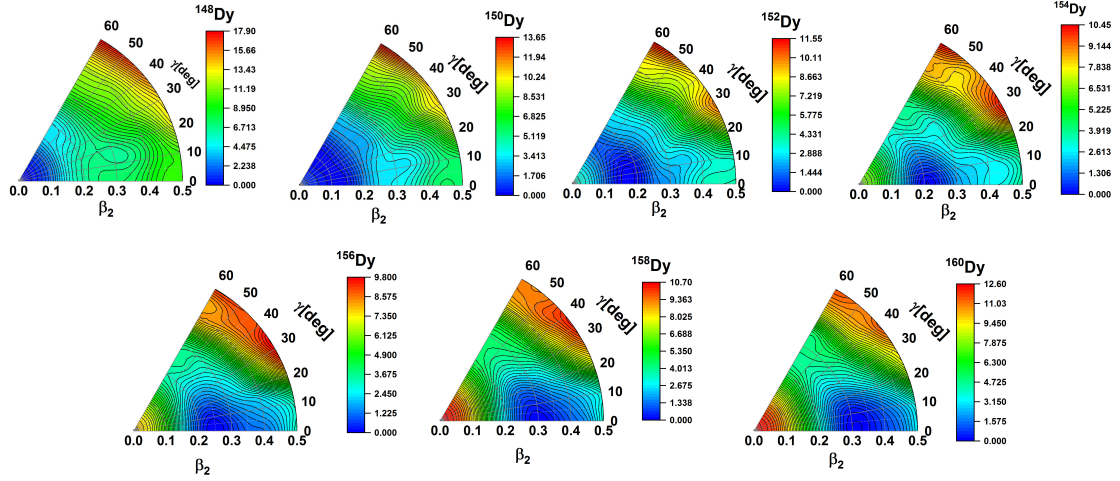
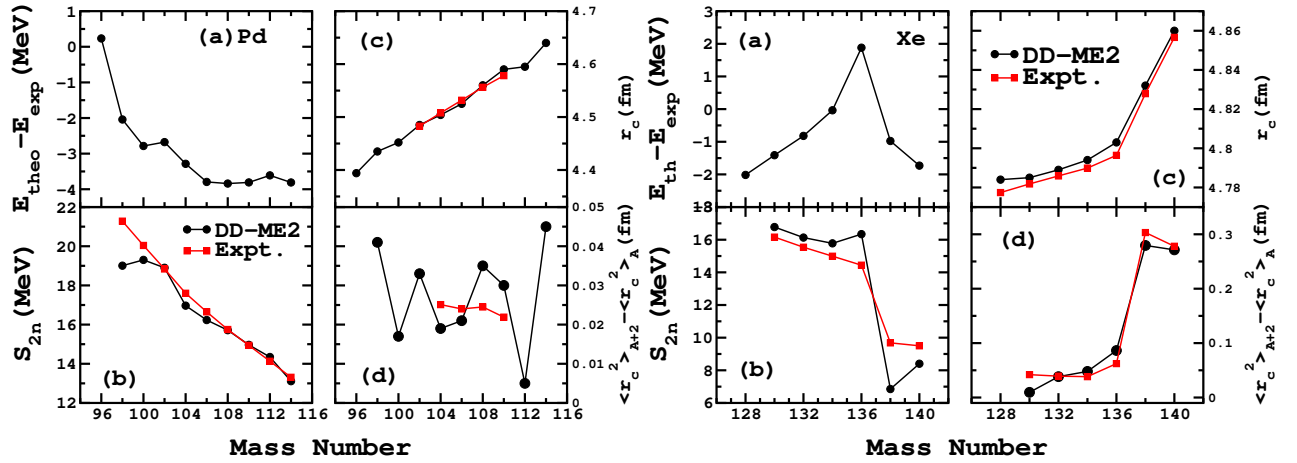


Figure 8. (Color online) Same as Fig.3 for the nuclei $^{146-158}\text{Gd}$.

Figure 9. (Color online) Same as Fig.3 for the nuclei $^{148-160}\text{Dy}$.Figure 10. (Color online) For Pd($Z=46$) and Xe($Z=54$) isotopes (a) Binding energy deviation from experimental data (b) Two-neutron separation energies S_{2n} (c) root-mean square charge radii r_c , and (d) isotopic shifts of the ground state charge radii. Comparison is made with the available experimental data.

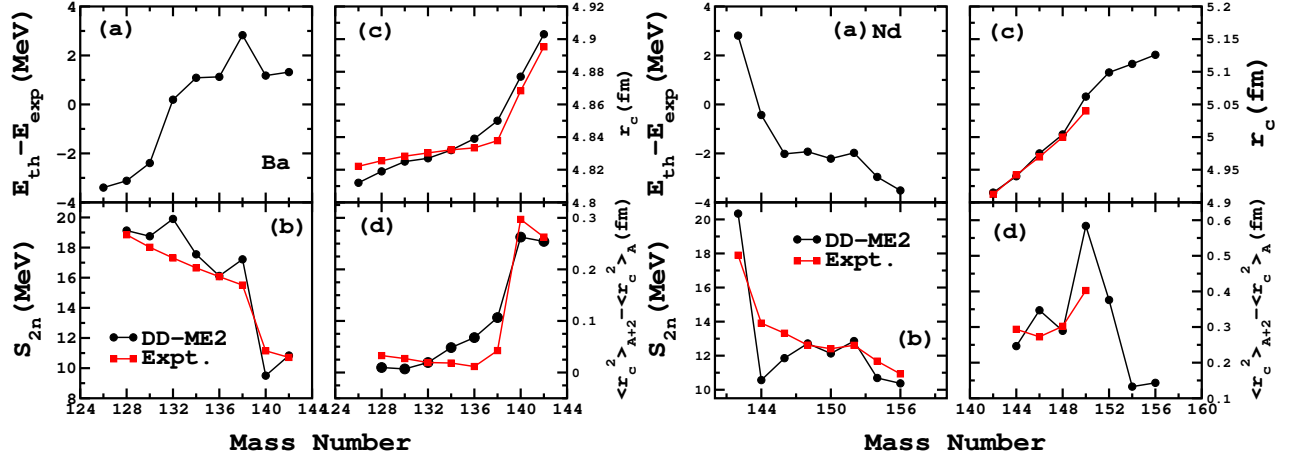


Figure 11. (Color online) Same as Fig.10 but for Ba(Z=56) and Nd(Z=60) isotopes.

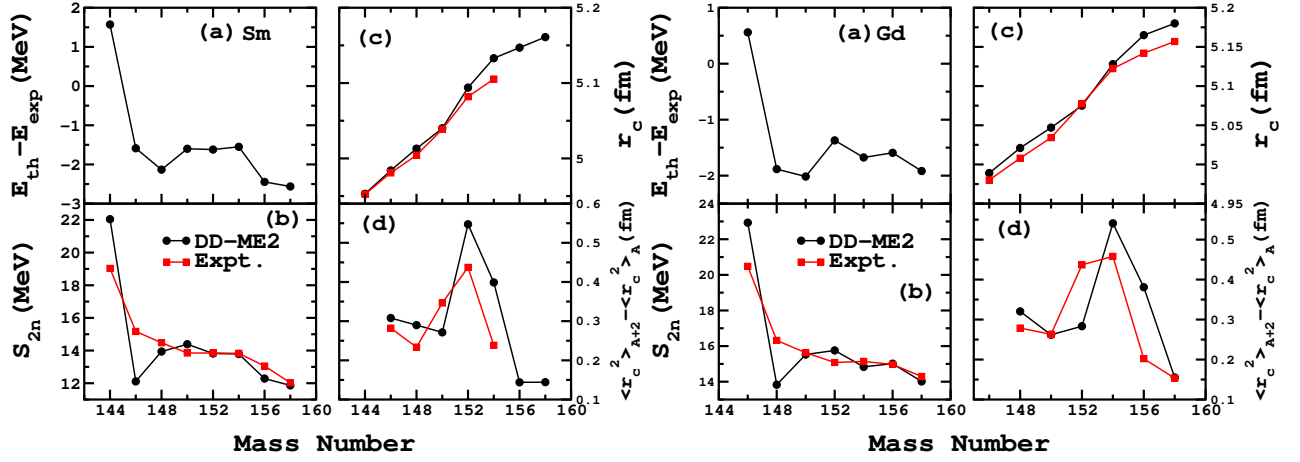


Figure 12. (Color online) Same as Fig.10 but for Sm(Z=62) and Gd(Z=64) isotopes.

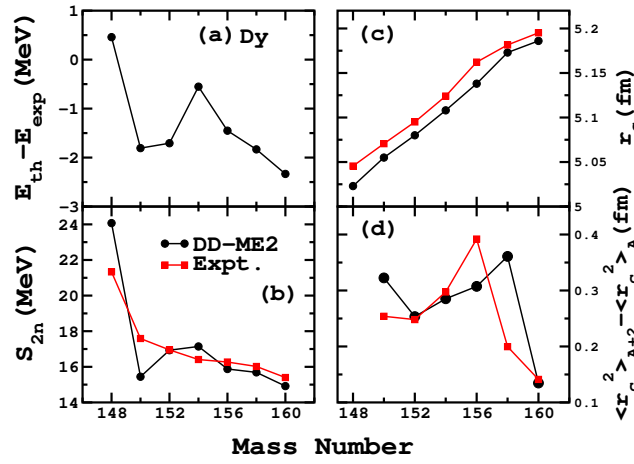


Figure 13. (Color online) Same as Fig.10 but for Dy(Z=66) isotopes.

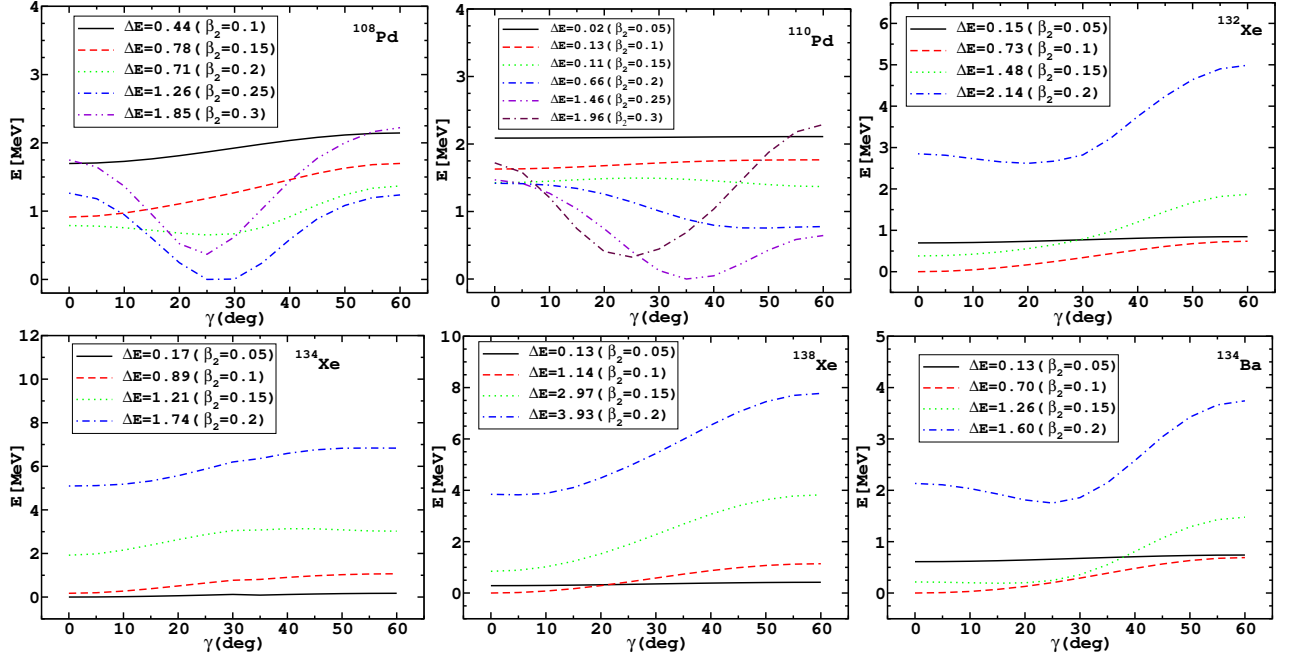


Figure 14. (Color online) Binding energy curves of the nuclei $^{108,110}\text{Pd}$, $^{132,134,138}\text{Xe}$, and ^{134}Ba as functions of the deformation parameter γ , for fixed values of axial deformation(β_2) with the DD-ME2 parameter set.

^{154}Gd and ^{156}Dy . The present results agree qualitatively with earlier theoretical [31, 32, 46, 81], and experimental studies [38, 40, 44, 45].

The dependency on the triaxial parameter(γ) is an important investigation for such cases. In order to check the properties of γ -dependence for E(5) symmetry in these nuclei, we have plotted the energy curves as a function of γ -variable for fixed values of β_2 . The results are shown in Fig. 14. Here ΔE is the energy difference between the minimum and maximum energy from $\gamma = 0^\circ$ to $\gamma = 60^\circ$ for fixed β_2 . Out of the possible E(5) candidates of Xe-isotopes, we can see that, $^{132,134}\text{Xe}$ are showing a weak dependence on γ for $0.05 \leq |\beta_2| \leq 0.2$ than ^{138}Xe . In case of Pd-isotopes, both the $^{108,110}\text{Pd}$ show weaker γ -dependence for $0.05 \leq |\beta_2| \leq 0.3$. Similarly, the negligible dependence on the γ -variable is found in ^{134}Ba . Therefore, we can say that, $^{108,110}\text{Pd}$, $^{132,134}\text{Xe}$, and ^{134}Ba could be suitable candidates to look for E(5) critical-point symmetry. Further, in case of X(5) symmetry, for a more clear picture of the γ dependence, we have plotted the energy as a function of γ for the fixed values of β_2 in Fig. 15. A clear indication of strong γ -dependence can be seen from Fig. 15. However, there is an almost gradual increase in energy with the increase in γ for ^{156}Dy up to $\gamma = 55^\circ$ above which it remains constant. From the above discussion, it is evident that in the present calculations, N=90 isotopes do not show a flat PESs, and ^{150}Nd , $^{150,152}\text{Sm}$, ^{154}Gd , and ^{156}Dy are possible candidates for X(5) critical-point symmetry. Qualitatively, this is in agreement with earlier calculations [31, 32, 35, 46, 47].

3.2. TPSM Results

In order to probe the high-spin properties of Dy, Gd, Sm, Nd, Pd, Xe and Ba isotopes, TPSM calculations have been performed with the basis deformation values chosen close to those obtained in the previous section. The variation in the deformations is justified as the two models employ very different Hamiltonian and the configuration spaces. What was noted that the axial deformations obtained in the previous section, don't require any major modifications, however, the non-axial deformation in the TPSM analysis needed readjustments to reproduce the γ bandhead energies. The deformation values used in the TPSM study are provided in Table 3.

TPSM study of the spectroscopic properties of atomic nuclei proceeds in several stages. In the first stage, the deformations listed in Table 3 are used to solve the three-dimensional Nilsson potential. The wave functions of this potential form the intrinsic basis functions in the TPSM approach. We would like to mention that, in principle, the basis functions with arbitrary deformation values can be used. However, optimum deformation values, which are

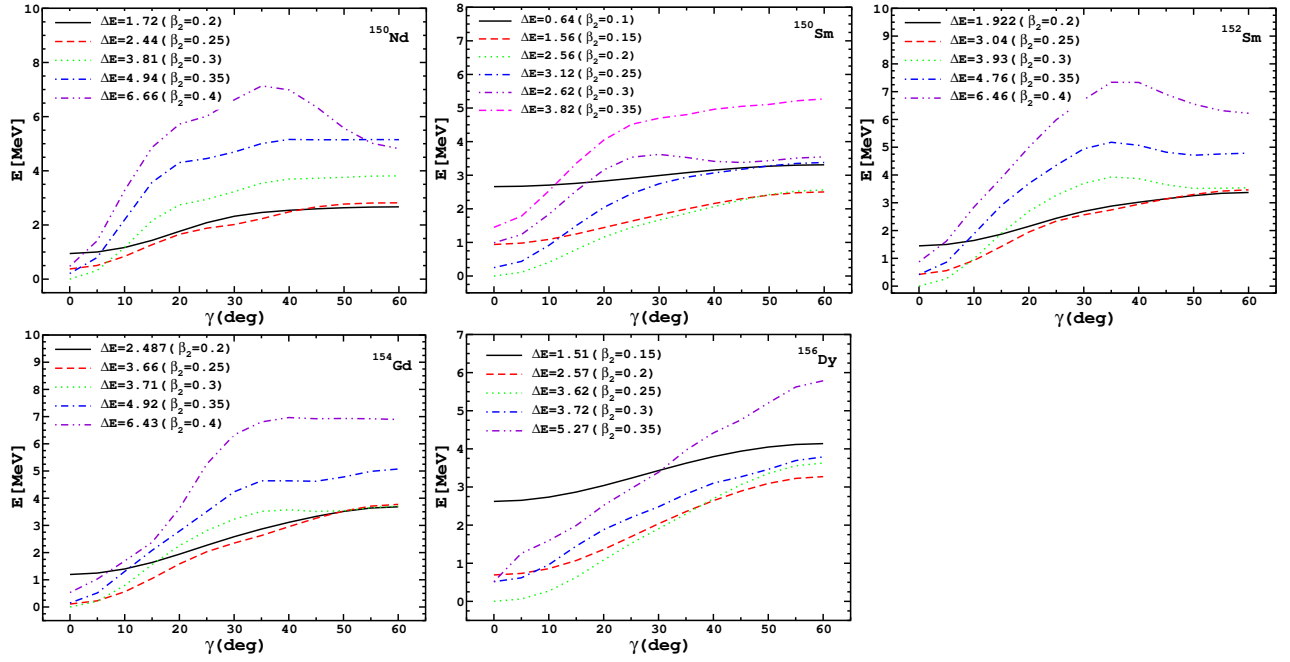


Figure 15. (Color online) Binding energy curves of the nuclei ^{150}Nd , $^{150,152}\text{Sm}$, ^{154}Gd , and ^{156}Dy as functions of the deformation parameter γ , for fixed values of axial deformation (β_2) with the DD-ME2 parameter set.

close to the expected deformation of the system, are employed so that a small window of the basis states are chosen for the diagonalization of the shell model Hamiltonian. In the present work, an energy window containing about 40 basis states has been selected for all the nuclei studied.

Table 3. Axial and triaxial quadrupole deformation parameters β and γ employed in the TPSM calculation for ^{156}Dy , ^{154}Gd , $^{150,152}\text{Sm}$, $^{150,156}\text{Nd}$, $^{102,108}\text{Pd}$, $^{132,134}\text{Xe}$ and ^{134}Ba isotopes.

	^{156}Dy	^{154}Gd	^{150}Sm	^{152}Sm	^{150}Nd	^{154}Nd	^{102}Pd	^{108}Pd	^{132}Xe	^{134}Xe	^{134}Ba
β	0.29	0.3	0.20	0.30	0.30	0.30	0.20	0.25	0.10	0.10	0.10
γ	20	19	22	19	20	19	20	22	20	20	20

In the second stage, the deformed basis states are projected onto good angular momentum states using the explicit three-dimensional angular momentum projection technique. In the third and final stage, these projected states are used to diagonalize the shell model given in section-2.2. Calculated energies for yrast and the γ bands for ^{156}Dy , ^{154}Gd , $^{150,152}\text{Sm}$, $^{150,156}\text{Nd}$, $^{102,108}\text{Pd}$, $^{132,134}\text{Xe}$ and ^{134}Ba are compared with the available experimental data in Fig. 16. It is quit evident from the results that TPSM calculations reproduce the experimental energies reasonably well.

In order to explore whether nuclei, under study, are γ -rigid or soft, odd-even staggering parameter defined as :

$$S(I) = \frac{E(I) - (E(I-1) + E(I+1))/2}{E(2_1^+)}, \quad (6)$$

is plotted in Fig. 17 for the γ bands. It is known that phenomenological Davydov-Filippov and Wilets-Jean potentials belonging to γ -rigid and γ -soft limits, respectively, give rise to similar excitation spectra for the ground-state band [82, 83]. Hence, it is not possible to separate the two limiting cases from the ground-state properties. However, it has been demonstrated that energy staggering, $S(I)$, in the γ -band may provide information on the nature of the γ -motion. It is shown that [84, 85] in case of γ -rigid, odd-spin values are favored as compared to the even-spin members and for γ -soft case it is opposite. It is evident from the two staggering figures that in all the nuclei, except for ^{152}Sm , even-spin states are lower than the odd-spin states, implying that all these nuclei are γ -soft. In the case of ^{152}Sm , the staggering

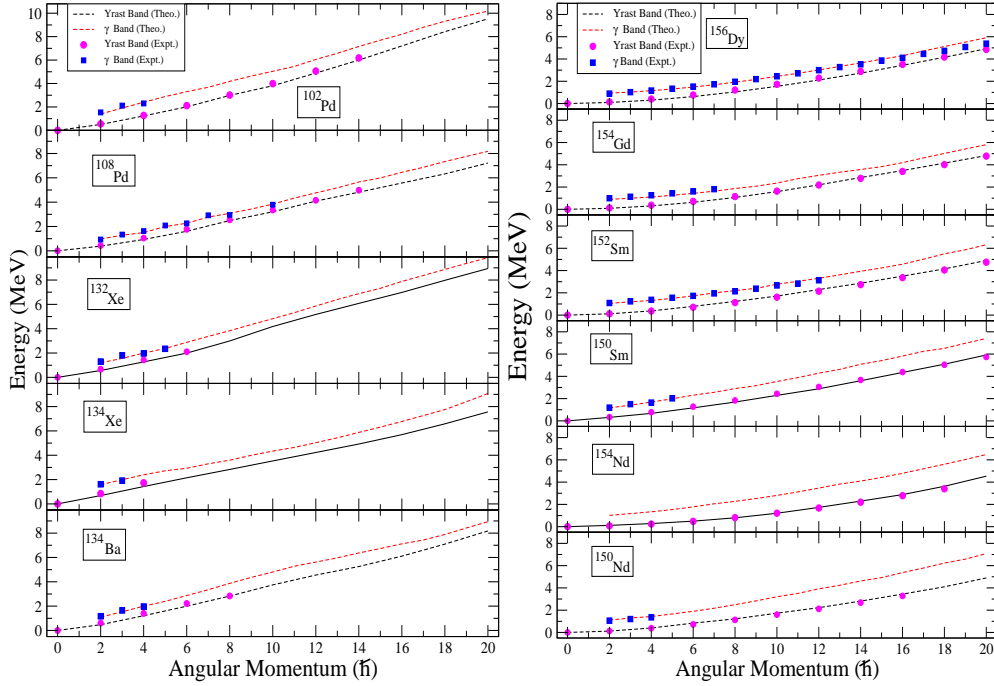


Figure 16. (Color online) Comparison of experimental and the calculated band energies for Pd, Xe, Ba, Dy, Gd, Sm, and Nd-isotopes. (Data taken from Refs. [86]–[94].)

parameter is quite small for low-spin states and it is not possible to make any statement regarding γ nature of these states. However, for high-spin states beyond $I=8$, odd-spin states are lower than even-spin states, indicating that this nucleus at high-spin has γ -rigid character.

The electromagnetic transition probabilities have also been studied in the present work using the expressions published in the earlier work [95]. The calculated BE2 transitions for the yrast and the γ bands are displayed in Figs. 18 and 19. In these figures, the available measured have also been plotted for a comparison. In most of the nuclei, a drop in BE2 is observed between $I=12$ –16, and is due to the rotation alignment of two-neutrons in the $i_{13/2}$ orbital. BE2 transitions for the γ -band also depict structural changes due to the crossing of the γ -band based on aligned two-quasiparticle configuration as discussed in our earlier work [96]. However, there is no experimental data available to compare with our theoretical predictions.

4. Conclusion

In the present calculations, we have investigated PESs for transitional nuclei $^{96-114}\text{Pd}$, $^{128-140}\text{Xe}$, and $^{126-138}\text{Ba}$, $^{142-156}\text{Nd}$, $^{144-158}\text{Sm}$, $^{146-158}\text{Gd}$ and $^{148-160}\text{Dy}$. In this paper, we have searched for the structural evolution with the increase of number of neutrons and protons within the isotopic/isotonic chains. We have also searched for the possible candidates that exhibit E(5) and X(5) critical-point symmetry behaviour at the critical point of the shape transition. The self-consistent RHB formalism with DD-ME2 force has been used. The analysis of the structural evolution is done on the basis of the evolution of the ground state shapes located within the axial potential energy surface calculations. It is further boosted by the triaxial calculations. The shape transition from spherical to deformed shape manifest themselves in a very clear manner in almost all the isotopic chains. Shape coexistence as well as the triaxial character is also observed. The calculations of the properties corresponding to the triaxial global minimum reproduces the experimental data very well. Based on the behaviour of the axial potential energy surface and further supported by the γ -dependence with the triaxial calculations, we have found that, $^{108,110}\text{Pd}$, $^{132,134}\text{Xe}$ and ^{134}Ba are suitable candidates to look for E(5) critical-point symmetry which have been suggested by earlier studies as examples of E(5) symmetry. We do not find ^{102}Pd as a possible candidate for E(5), contradicting some earlier predictions [21, 23, 31],

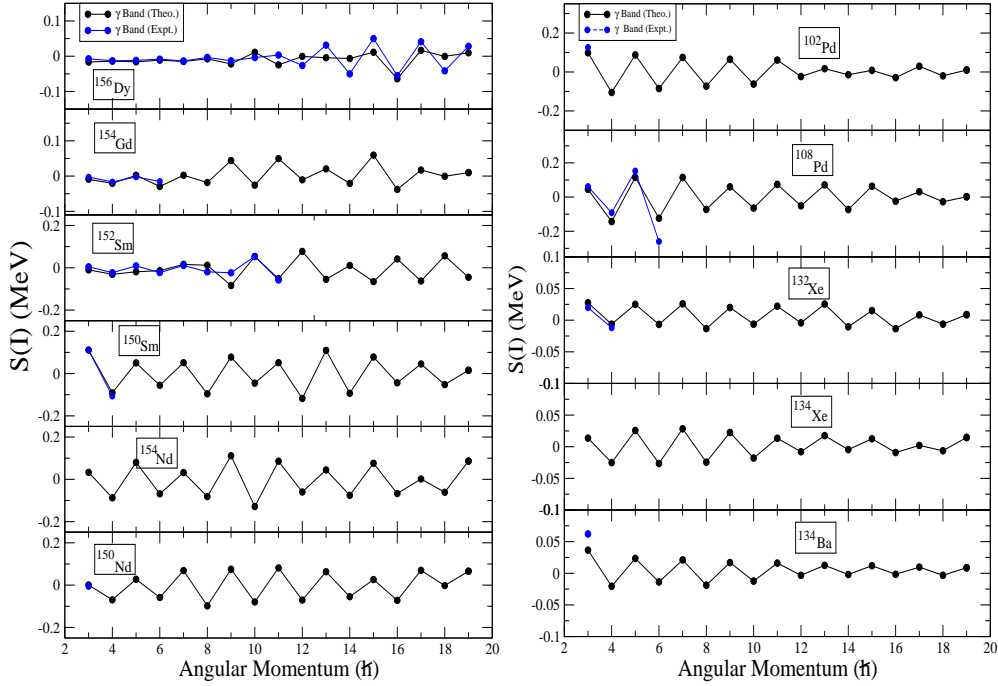


Figure 17. (Color online) Comparison of observed and TPSM calculated staggering parameter 6 for the γ -band in ^{156}Dy [94], ^{154}Gd [93], $^{150,152}\text{Sm}$ [91, 92], $^{150,154}\text{Nd}$ [91, 93], $^{102,108}\text{Pd}$ [86, 87], $^{132,134}\text{Xe}$ [88, 89], and ^{134}Ba [89].

but, in agreement with the very recent experiment for ^{102}Pd through Recoil Distance Doppler Shift(RDDS) [36] measurement. The isotopes ^{150}Nd , ^{152}Sm and ^{154}Gd are found to be good candidates while ^{150}Sm and ^{156}Dy are poor candidates of X(5) critical-point symmetry. Triaxial projected shell model has also been employed to study band structures in this work. The TPSM calculation for yrast and γ -band energy produces the experimental results. Through the analysis of the γ -band and the staggering, it has been shown that all the nuclei, except for ^{152}Sm are γ -soft at high spin.

5. Acknowledgement

S. Ahmad would like to thank the Inter-University Accelerator Centre (IUAC), New Delhi for providing the High Performance Computing Facility (HPC) at IUAC.

References

- [1] F. Iachello, Phys. Rev. Lett. **85**, 3580 (2000).
- [2] F. Iachello, Phys. Rev. Lett. **87**, 052502 (2001).
- [3] A. Bohr and B. R. Mottelson, *Nuclear Structure*(Benjamin, New York, 1975).
- [4] R.F. Casten, D. Kusnezov, N.V. Zamfir, Phys. Rev. Lett. **82**, 5000 (1999).
- [5] R. F. Casten and N. V. Zamfir, Phys. Rev. Lett. **85**, 3584 (2000).
- [6] R.F. Casten and N.V. Zamfir, Phys. Rev. Lett. **87**, 052503 (2001).
- [7] R.F. Casten, N.V. Zamfir, and R. Krucken, Phys. Rev. C **68**, 059801 (2003).
- [8] R.F. Casten, Nature Phys. **2**, 811 (2006).
- [9] R.F. Casten and E. A. McCutchan, J. Phys. G **34**, R285 (2007).
- [10] J. Jolie, P. Cejnar, J. Dobes, Phys. Rev. C **60**, 0613003 (1999).
- [11] J. Jolie, R.F. Casten, P. von Brentano, V. Werner, Phys. Rev. Lett. **87**, 162501 (2001).
- [12] J. Jolie, P. Cejnar, R.F. Casten, S. Heinze, A. Linnemann, V. Werner, Phys. Rev. Lett. **89**, 182502 (2002).
- [13] J. Jolie and R.F. Casten, Nucl. Phys. News **15**, 20 (2005).
- [14] P. Cejnar and J. Jolie, *Progress in Particle and Nuclear Physics*, **62**, 210 (2009).
- [15] P. Cejnar, J. Jolie, and R. F. Casten, Rev. Mod. Phys. **82**, 2155 (2010).

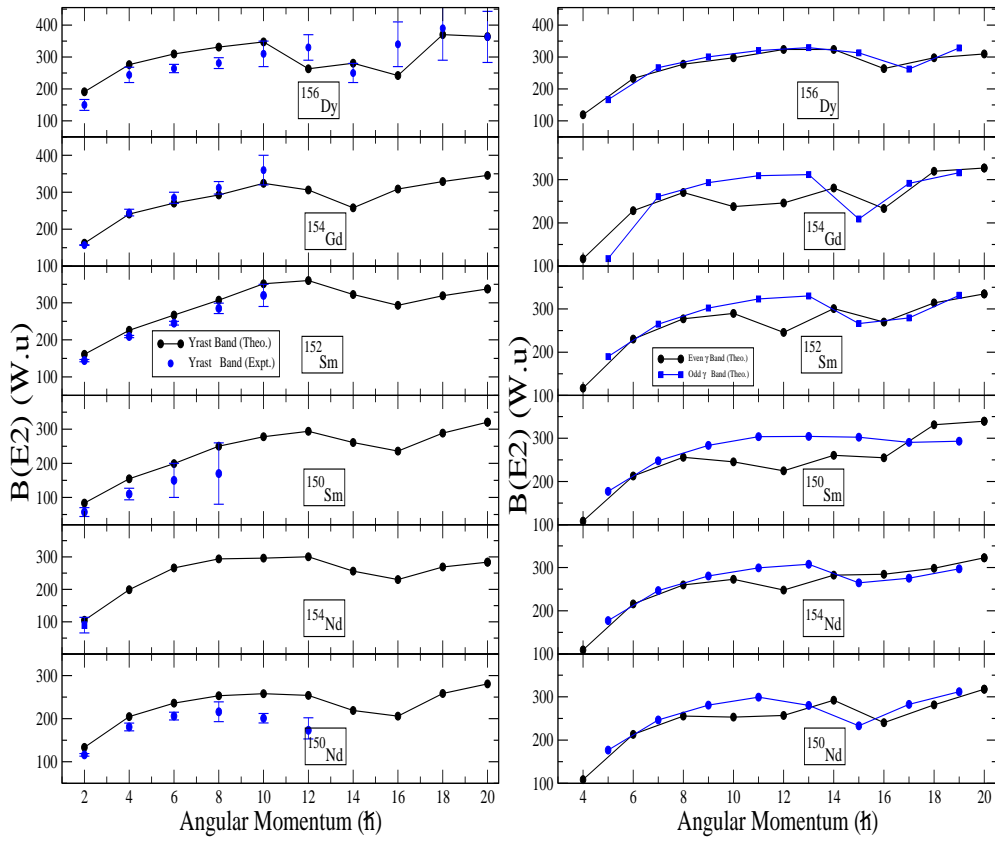


Figure 18. (Color online) Calculated $B(E2)$ transition probabilities for the ground state bands (left panel) and γ -bands (right panel) using TPMSM approach. The experimental values have been taken from Ref. [86]–[94].

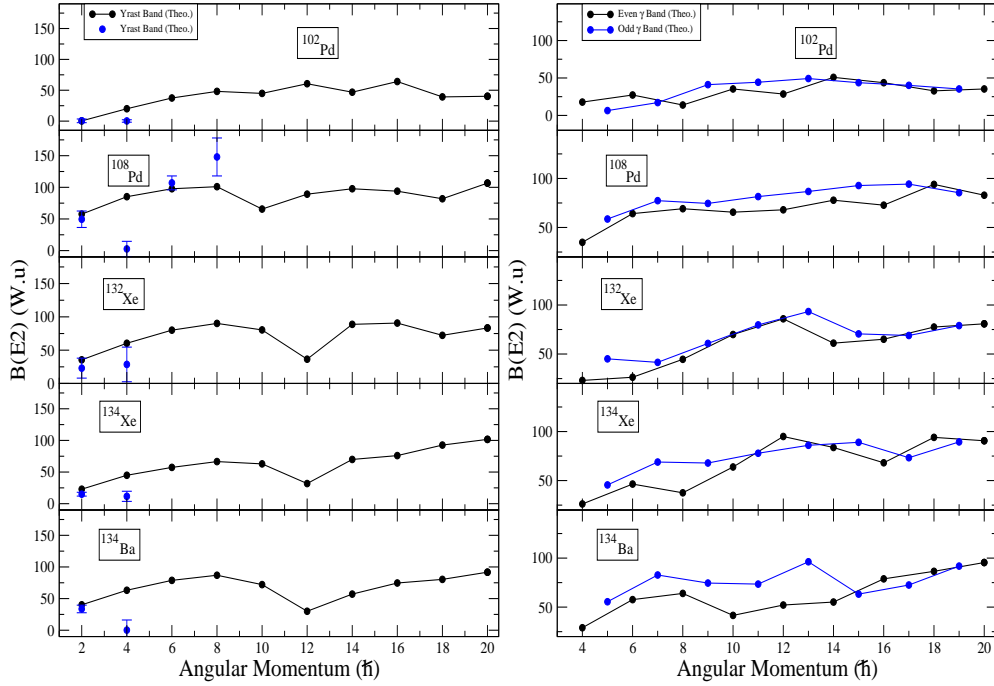


Figure 19. (Color online) Calculated $B(E2)$ transition probabilities for the ground state bands (left panel) and γ -bands (right panel) using TPSPM approach. The experimental values have been taken from Refs. [86]–[94].

- [16] N. Shimizu, T. Otsuka, T. Mizusaki, and M. Honma, Phys. Rev. Lett. **86**, 1171 (2001).
- [17] V. Werner, P. von Brentano, R.F. Casten, J. Jolie, Phys. Lett. B **527**, 55 (2002).
- [18] M.A. Caprio et al., Phys. Rev. C **66**, 054310 (2002).
- [19] T. Niksic, D. Vretenar, G. A. Lalazissis, and P. Ring, Phys. Rev. Lett. **99**, 092502 (2007).
- [20] J. M. Arias, Phys. Rev. C **63**, 034308 (2001).
- [21] N. V. Zamfir et al., Phys. Rev. C **65**, 044325 (2002); 067305 (2002).
- [22] N. V. Zamfir et al., Phys. Rev. C **65**, 067305 (2002).
- [23] R. M. Clark et al., Phys. Rev. C **69**, 064322 (2004).
- [24] R. M. Clark et al., Phys. Rev. C **67**, 041302(R) (2003).
- [25] R. Bijker, R. F. Casten, N. V. Zamfir, and E. A. McCutchan, Phys. Rev. C **68**, 064304 (2003); **69**, 059901(E) (2004).
- [26] M.W. Kirson, Phys. Rev. C **70**, 049801(2004).
- [27] U. Kneissl, in *Key topics in Nuclear Structures(paestum 2004)*, edited by A. Covello (World Scientific, Singapore, 2005), p.399.
- [28] D.-L. Zhang and H.-Y. Zhao, Chin. Phys. Lett. **19**, 779 (2002).
- [29] D.-L. Zhang and Y.-X. Liu, Phys. Rev. C **65**, 057301 (2002).
- [30] D.-L. Zhang and Y.-X. Liu, Chin. Phys. Lett. **20**, 1028 (2003).
- [31] R. Fossion, D. Bonatsos and G. A. Lalazissis, Phys. Rev. C **73**, 044310 (2006).
- [32] R. Rodríguez-Guzman and P. Sarriguren, Phys. Rev. C **76**, 064303 (2007).
- [33] Z. P. Li, T. Niksic, D. Vretenar, J. Meng, G. A. Lalazissis, and P. Ring, Phys. Rev. C **79**, 054301 (2009).
- [34] Z. P. Li, T. Niksic, D. Vretenar, and J. Meng, Phys. Rev. C **80**, 061031(R) (2009).
- [35] Z. P. Li, T. Niksic, D. Vretenar and J. Meng, Phys. Rev. C **81**, 034316 (2010).
- [36] T. Konstantinopoulos et al., Phys. Rev. C **93**, no. 1, 014320 (2016).
- [37] E. E. Peters et al., Phys. Rev. C **94**, no. 2, 024313 (2016).
- [38] R. Krucken et al., Phys. Rev. Lett. **88**, 232501 (2002).
- [39] R. F. Casten and N. V. Zamfir, Phys. Rev. Lett. **87**, 052503 (2001).
- [40] J. B. Gupta and J. H. Hamilton, Phys. Rev. C **96**, no. 3, 034321 (2017).
- [41] T. Togashi, Y. Tsunoda, T. Otsuka, and N. Shimizu, Phys. Rev. Lett. **117**, 172502 (2016).
- [42] K. Nomura, T. Niksic and D. Vretenar, Phys. Rev. C **96**, 014304 (2017).
- [43] D. Tonev et al., Phys. Rev. C **69**, 034334 (2004).
- [44] A. Dewald et al., Eur. Phys. J. A **20**, 173 (2004).
- [45] O. Moller et al., Phys. Rev. C **74**, 024313 (2006).
- [46] J. Meng, W. Zhang, S. G. Zhou, H. Toki, and L. S. Geng, Eur. Phys. J. A **25**, 23 (2005).
- [47] Z.-Q. Sheng and J.-Y. Guo, Mod. Phys. Lett. A **20**, 2711 (2005).
- [48] T. R. Rodriguez and J. L. Egido, Phys. Lett. B **663**, 49 (2008).

- [49] L. M. Robledo, R. Rodríguez-Guzman and P. Sarriguren, Phys. Rev. C **78**, 034314 (2008).
- [50] G. A. Lalazissis, T. Nikšić, D. Vretenar, and P. Ring, Phys. Rev. C **71**, 024312 (2005).
- [51] S. E. Agbemava, A. V. Afanasjev, D. Ray, and P. Ring, Phys. Rev. C, **89**, 054320 (2014).
- [52] S. E. Agbemava, A. V. Afanasjev, D. Ray, and P. Ring, Phys. Rev. C, **95**, 054324 (2017).
- [53] A. V. Afanasjev and S. E. Agbemava, Phys. Rev. C **93**, 054310 (2016).
- [54] S. E. Agbemava, A. V. Afanasjev, T. Nakatsukasa, and P. Ring, Phys. Rev. C **92**, 054310 (2015).
- [55] T. Nikšić, D. Vretenar, and P. Ring, Phys. Rev. C **78**, 034318 (2008).
- [56] T. Nikšić, D. Vretenar, P. Finelli, and P. Ring, Phys. Rev. C **66**, 024306 (2002).
- [57] X. Roca-Maza, X. Viñas, M. Centelles, P. Ring, and P. Schuck, Phys. Rev. C **84**, 054309 (2011).
- [58] N. Paar, D. Vretenar, E. Khan and G. Coló, Rep. Prog. Phys. **70**, 691 (2007).
- [59] H. Abusara, Shakeb Ahmad, Phys. Rev. C **96**, 064303 (2017).
- [60] H. Abusara, Shakeb Ahmad, and S. Othman, Phys. Rev. C **95**, 054302 (2017).
- [61] Afaq Karim, Shakeb Ahmad, Phys. Rev. C **92**, 064608 (2015).
- [62] H. Abusara, A. V. Afanasjev, and P. Ring, Phys. Rev. C **85**, 024314 (2012).
- [63] T. Nikšić, D. Vretenar, and P. Ring, Prog. Part. Nucl. Phys. **66**, 519 (2011).
- [64] A. V. Afanasjev and H. Abusara, Phys. Rev. C **81**, 014309 (2010).
- [65] D. Vretenar, A. V. Afanasjev, G. A. Lalazissis, and P. Ring, Phys. Rep. **409**, 101 (2005).
- [66] Y. K. Gambhir, P. Ring, and A. Thimet, Ann. Phys. (NY) **198**, 132 (1990).
- [67] P. Ring and P. Schuck, *The Nuclear Many-Body Problem*, eds. W. Beiglbock et al. (New York, Springer-Verlag), (1980).
- [68] W. Koepf and P. Ring, Nucl. Phys. **A493**, 61 (1989).
- [69] T. Nikšić, N. Paar, D. Vretenar, and P. Ring, Comp. Phys. Comm. **185**, 1808 (2014).
- [70] P. Ring, Prog. Part. Nucl. Phys. **37**, 193 (1996).
- [71] Nikšić, P. Ring, D. Vretenar, Y. Tian, Z. Y. Ma, Phys. Rev. C **81**, 054318 (2010).
- [72] J. A. Sheikh, G. H. Bhat, W. A. Dar, S. Jehangir and P. A. Ganai, Phys. Scr. **91**, 063015 (2016).
- [73] S. Jehangir, G.H. Bhat, J.A. Sheikh, R. Palit, and P.A. Ganai, Nuclear Physics **A 968**, 48 (2017).
- [74] J. A. Sheikh and K. Hara, Phys. Rev. Lett. **82**, 3968 (1999).
- [75] Y. Sun, K. Hara, J. A. Sheikh, J. G. Hirsch, V. Velazquez, and M. Guidry, Phys. Rev. C **61**, 064323 (2000).
- [76] J. A. Sheikh, Y. Sun, and R. Palit, Phys. Lett. **B 507**, 115 (2001).
- [77] Y. Sun, J. A. Sheikh, and G.-L. Long, Phys. Lett. **B 533**, 253 (2002).
- [78] J. A. Sheikh, G. H. Bhat, Y. Sun, G. B. Vakil, and R. Palit, Phys. Rev. C **77**, 034313 (2008).
- [79] J. A. Sheikh, G. H. Bhat, R. Palit, Z. Naik, and Y. Sun, Nucl. Phys. **A 824**, 58 (2009).
- [80] K. Hara and Y. Sun, Int. J. Mod. Phys. **E 4**, 637 (1995).
- [81] J.-Y. Zhang, M. A. Caprio, N. V. Zamfir, and R. F. Casten, Phys. Rev. C **60**, 061304(R) (1999).
- [82] A.S. Davydov and G. P. Filippov, Nucl. Phys. **8**, 237 (1958).
- [83] L. Wilets and M. Jean, Phys. Rev. **102**, 788 (1956).
- [84] N.V. Zamfir and R.F. Casten, Phys. Lett. **B 260**, 265 (1991).
- [85] E.A. McCutchan et al., Phys. Rev. **C76**, 024306 (2007).
- [86] P.De Gelder, D.De Frenne and E.Jacobs, Nucl. Data Sheets **35**, 443 (1982).
- [87] Jean Blachot Nucl. Data Sheets **91**, 135 (2000).
- [88] H.R.Hiddleston and C.P.Browne Nucl. Data Sheets **17**, 225 (1976).
- [89] Yu. V.Sergeenkov and V.M.Sigalov, Nucl. Data Sheets **34**, 475 (1981).
- [90] L.K.Peker, Nucl. Data Sheets **36**, 289 (1982).
- [91] S.K.Basu and A.A.Sonzogni, Nucl. Data Sheets **114**, 435 (2013).
- [92] L.K.Peker, Nucl. Data Sheets **58**, 93 (1989).
- [93] C.W.Reich, Nucl. Data Sheets **110**, 2257 (2009).
- [94] C.W.Reich, Nucl. Data Sheets **113**, 2537 (2012).
- [95] S. Jehangir, G. H. Bhat, J. A. Sheikh, R. Palit and P. A. Ganai, Nuc. Phys. **A 968**, 48 (2017).
- [96] S. Jehangir et al., Phys. Rev. C **97**, 014310 (2018).